

# Measuring a cosmological distance–redshift relationship using only gravitational wave observations of binary neutron star coalescences

C. Messenger

*School of Physics and Astronomy, Cardiff University, Queens Buildings, The Parade, Cardiff, CF24 3AA\**

J. Read

*Department of Physics and Astronomy, The University of Mississippi, P.O. Box 1848, Oxford, Mississippi 38677-1848*

(Dated: Mon Jul 25 14:42:23 2011 +0100)

(commitID: eeee4860739fb3b67cad45b78621230519b0c9f0)

Detection of gravitational waves from the inspiral phase of binary neutron star coalescence will allow us to measure the effects of the tidal coupling in such systems. These effects will be measurable using 3<sup>rd</sup> generation gravitational wave detectors, e.g. the Einstein Telescope, which will be capable of detecting inspiralling binary neutron star systems out to redshift  $z \approx 4$ . Tidal effects provide additional contributions to the phase evolution of the gravitational wave signal that break a degeneracy between the system’s mass parameters and redshift and thereby allowing for the simultaneous measurement of both the effective distance and the redshift for individual sources. Using the population of  $O(10^3-10^7)$  detectable binary neutron star systems predicted for the Einstein Telescope the luminosity distance–redshift relation can be probed independently of the cosmological distance ladder and independently of electromagnetic observations. We present the results of a Fisher information analysis applied to waveforms assuming a subset of possible neutron equations of state. We conclude that the redshift of such systems can be determined to  $O(10\%)$  for  $z > 1$  and in the most optimistic case accuracies of 2% can be achieved.

PACS numbers: 26.60.Kp, 95.85.Sz, 98.80.-k, 98.62.Py

Keywords: neutron stars, gravitational waves, cosmology

*Introduction*— Making use of gravitational-wave (GW) sources as standard sirens (the GW analogue of electromagnetic (EM) standard candles) was first proposed in [1]. It was noted that the amplitude of a GW signal from the coalescence of a compact binary such as a binary neutron star (BNS) is a function of the redshifted component masses and the luminosity distance. Since the former can be estimated separately from the signal phase evolution, the luminosity distance can be extracted and such systems can be treated as self-calibrating standard sirens. This indicated that GW observations do not require the cosmological distance ladder to measure distances but concluded that EM observations would be needed to measure the redshift of GW sources. Upon detection of a GW signal from a compact binary coalescence, one could localize the source on the sky using a network of GW detectors. The host galaxy of the source could then be identified and used to obtain accurate redshift information whilst inferring the luminosity distance from the GW amplitude. This idea that GW and EM observations could complement each other in this way was subsequently extended to include the fact that BNS events are now thought to be the progenitors of most “short-hard” Gamma-Ray bursts (GRBs) [2]. The expected temporal coincidence of these events would allow the more accurately measured sky position of the GRB to be used to identify the host galaxy. Recent work [3–5] has explored the technical details regarding the data analysis of BNS standard sirens with respect to the advanced and 3<sup>rd</sup> generation GW detectors with the aim of investigating the potential of GW observations as tools for performing precision cosmology.

The operation of the initial generation of interferomet-

ric GW detectors has been successfully completed. This comprised a network of four widely-separated Michelson interferometers: the Laser Interferometer Gravitational-wave Observatory (LIGO) detectors [6] in Washington and Louisiana, USA, GEO 600 [7] in Hannover, Germany and Virgo [8] in Cascina, Italy. We now await the construction of the advanced detectors [9] which will recommence operations in ~2015 and promise to provide the first direct detection of GWs. It is expected that in this advanced detector era the most likely first detections will be from compact binary coalescences of BNS systems. Astrophysical estimates suggest a rate of detection of at least a few, and possibly a few dozen, per year [10] with typical signal-to-noise-ratio (SNR)  $O(10)$ . Already much effort has been spent on the design of a 3<sup>rd</sup> generation GW detector the Einstein Telescope (ET) [11] which is anticipated to be operational by ~2025. It is designed to be ~10 times more sensitive in GW strain than the advanced detectors and as such we would expect to detect  $O(10^3-10^7)$  BNS events per year [4, 10] with SNRs ranging up to  $O(100)$ .

In this letter we highlight an important feature associated with the information that we will be able to extract from BNS waveforms using 3<sup>rd</sup> generation GW interferometers, in particular ET [11]. We show that the addition of the tidal coupling contribution to the GW waveform breaks the degeneracy present in post-Newtonian (PN) waveforms between the mass parameters and the redshift. This will then allow the measurement of the binary rest-frame masses, the luminosity distance and redshift simultaneously for individual BNS events. We base our work on the assumption that the detections of BNS and black-hole–neutron star (BHNS) coalescences made using both the advanced detectors and ET

arXiv:1107.5725v1 [gr-qc] 28 Jul 2011

(specifically the nearby high SNR signals) would tightly constrain the universal NS core equation of state (EOS) [12–15]. Once the EOS is known, the tidal effects are completely determined by the component rest-frame masses of the system. Exploitation of these effects would then entirely remove the requirement for coincident EM observations (so-called “multi-messenger” astronomy) to obtain redshift information. In using GRB counterparts for example, host galaxy identification [16] can sometimes be unreliable. We also require that the light cone from the GRB is coincident with our line of sight. Current estimates of the half-opening angles of GRBs lie in the range 8–30° [17, 18], which coupled with the fact that only some short-hard GRBs have measured redshifts imply that only a small fraction ( $\sim 10^{-3}$ ) of BNS events will be useful as standard sirens. Removing the necessity for coincident EM observations will allow all of the  $\mathcal{O}(10^3\text{--}10^7)$  BNS events seen with ET to be assigned a redshift measure independent of sky position. Each of these detected events provides a measure of the luminosity distance–redshift relation ranging out to redshift  $z \approx 4$ . With so many potential sources the observed distribution of effective distance (the actual luminosity distance multiplied by a geometric factor accounting for the orientation of the binary relative to the detector) within given redshift intervals will allow the accurate determination of actual luminosity distance and consequently of cosmological parameters including those governing the dark energy equation of state. Such a scenario significantly increases the potential for 3<sup>rd</sup> generation GW detectors to perform precision cosmology with GW observations alone.

*The signal model*—We follow the approach of [19, 20] in our determination of the uncertainties in our inspiral waveform parameters. We use as our signal model the frequency domain stationary phase approximation [21] to the waveform of a non-spinning BNS inspiral,

$$\tilde{h}(f) = \sqrt{\frac{5}{24}} \pi^{-2/3} \mathcal{Q}(\varphi) \frac{\mathcal{M}^{5/6}}{r} f^{-7/6} e^{-i\Psi(f)}, \quad (1)$$

where we are using the convention  $c = G = 1$ . We define the total rest mass  $M = m_1 + m_2$  and the symmetric mass ratio  $\eta = m_1 m_2 / M^2$  where  $m_1$  and  $m_2$  are the component rest masses. The chirp mass  $\mathcal{M}$  is defined as  $\mathcal{M} = M \eta^{3/5}$  and  $r$  is the proper distance to the GW source. The quantity  $\mathcal{Q}(\varphi)$  is a factor that is determined by the amplitude response of the GW detector and is a function of the nuisance parameters  $\varphi = (\theta, \phi, \iota, \psi)$  where  $\theta$  and  $\phi$  are the sky position coordinates and  $\iota$  and  $\psi$  are the orbital inclination and GW polarization angles respectively. The standard post-Newtonian point particle frequency domain phase can be written as [20, 22]

$$\Psi_{PP}(f) = 2\pi f t_c - \phi_c - \frac{\pi}{4} + \frac{3}{128\eta x^{5/2}} \sum_{k=0}^N \alpha_k x^{k/2} \quad (2)$$

where we use the post-Newtonian dimensionless parameter  $x = (\pi M f)^{2/3}$  and the corresponding coefficients  $\alpha_k$  given in [20]. Throughout this work we use  $N = 7$  corresponding to a 3.5 PN phase expansion (the highest known at the

time of publication). The parameters  $t_c$  and  $\phi_c$  are the time of coalescence and phase at coalescence. We use  $f$  to represent the GW frequency in the rest frame of the source. Note that if the signal is modeled using the point-particle phase such that  $\Psi(f) = \Psi_{PP}(f)$  then the detected signal  $\tilde{h}(f)$  is invariant under the transformation  $(f, \mathcal{M}, r, t) \rightarrow (f/\xi, \mathcal{M}\xi, r\xi, t\xi)$ . For BNS systems at cosmological distances the frequency is redshifted such that  $f \rightarrow f/(1+z)$  where  $z$  is the source’s cosmological redshift. Therefore, using the point-particle approximation to the waveform one is only able to determine the “redshifted” chirp mass  $\mathcal{M}_z = (1+z)\mathcal{M}$  and the so-called luminosity distance  $d_L = (1+z)r$ . This implies that it is not possible to disentangle the mass parameters and the redshift from the waveform alone if the proper distance is unknown.

The additional phase contribution to a GW signal from a BNS system due to quadrupolar tidal interactions including all post-1-Newtonian effects is given by [12, 23]

$$\Psi^{\text{tidal}}(f) = \sum_{a=1,2} \frac{3\lambda_a}{128\eta} \left[ -\frac{24}{\chi_a} \left( 1 + \frac{11\eta}{\chi_a} \right) \frac{x^{5/2}}{M^5} - \frac{5}{28\chi_a} (3179 - 919\chi_a - 2286\chi_a^2 + 260\chi_a^3) \frac{x^{7/2}}{M^5} \right] \quad (3)$$

where we sum over the contributions from each neutron star (NS) (indexed by  $a$ ). The tidal deformability parameter for each NS  $\lambda = (2/3)R_{\text{ns}}^5 k_2$  is a function of the  $l = 2$  tidal Love number [14, 24] (apsidal constant)  $k_2$ . We have also defined  $\chi_a = m_a/M$ . Note that although the terms included in Eq. 3 are Newtonian and 1PN, they are formally of 5PN and 6PN since they have the same frequency dependences of  $x^{5/2}$  and  $x^{7/2}$ . However, their coefficients are of order  $(R_{\text{ns}}/M)^5 \sim 10^5$  making them comparable in magnitude with the 3PN and 3.5PN phasing terms.

For a chosen universal NS EOS the NS mass can be used to determine the NS radius  $R_{\text{ns}}$ , Love number  $k_2$  and therefore also the tidal deformability parameter  $\lambda_a$ . For the purposes of this work we use the relationship between the NS mass and the tidal deformability parameter expressed graphically in Fig. 2 of [12]. Our approach models this relationship as a first-order Taylor expansion around the canonical NS mass value such that  $\lambda(m) = \lambda_{1.4} + (d\lambda/dm)_{1.4}(m - 1.4M_{\odot})$  where  $\lambda_{1.4}$  and  $(d\lambda/dm)_{1.4}$  are the values of the tidal deformability parameter and its derivative with respect to mass, both evaluated at  $m = 1.4M_{\odot}$ .

We now highlight the fundamental feature of this work. With the addition of the tidal phase components to the total GW phase such that  $\Psi(f) = \Psi_{PP}(f) + \Psi^{\text{tidal}}(f)$  the waveform is no longer invariant under the type of transformation discussed above. The point-particle PN phase as measured at the detector is a function of the redshifted chirp mass  $\mathcal{M}_z$  and luminosity distance  $d_L$  in contrast to the tidal phase component which contains terms dependent upon the un-redshifted rest-frame mass components  $m_1$  and  $m_2$ . The degeneracy between the mass parameters and the redshift is therefore broken and one can now theoretically measure both sets of quantities independently of one another. Essentially, the NS size provides

a fixed scale-length that is imprinted on the GW waveform. The ability to perform this measurement is based on the assumption that one knows or has a very well constrained NS EOS. As shown in [15], in the advanced detector era, departures from the point-particle limit of the GW waveform as the stars approach their final plunge and merger will place strong constraints on the NS radius and consequently will also constrain the EOS. In the 3<sup>rd</sup> generation GW detector era, specifically the ET [11], the subset of high SNR BNS signals from local galaxies will provide even tighter constraints. The addition of future EM observational constraints on the EOS (as can be seen currently in [25, 26]) will also contribute to a well-understood NS EOS by the ET era.

The question of the upper cut-off frequency is also an important issue. The standard approach to tidal effects on GW waveforms has been to truncate the signal corresponding to a rest-frame GW frequency of 450 Hz. Such a choice has been made so as to limit the contributions to the phase evolution from various higher order effects to <10%. We note that in all studies where this cut-off frequency has been used only the leading order Newtonian tidal phase component has been included. With the addition of the 1PN tidal phase correction, and neglecting the small known higher-multipole contributions [27], the tidal description is limited by nonlinear and resonant tidal effects [28] at the end of inspiral. Concurrently, the PN formalism is also breaking down at the innermost-stable-circular orbit (ISCO) frequency  $f_{\text{isco}} = (6^{3/2}\pi M)^{-1}$  ( $\sim 1500$  Hz for  $1.4M_{\odot}$  BNS systems) where the secular approximation, that the mode frequency is large compared to the orbit frequency, also becomes invalid. We compute our results for both conservative 450 Hz and more optimistic ISCO cutoff frequencies, producing results that can be assumed as bracketing a realistic scenario. We note that this upper cut-off frequency is applied using un-redshifted mass in the source's local frame, or equivalently using redshifted mass in the detector's frame.

The standard Fisher matrix formalism [29, 30] allows us to compute the uncertainties associated with the measurement of a set of signal parameters. In the large SNR regime under the assumption of Gaussian noise the signal parameters  $\theta$  have probability distribution  $p(\theta) \propto \exp(-(1/2)\Gamma_{ij}\delta\theta^i\delta\theta^j)$ , where  $\delta\theta^i = \theta^i - \hat{\theta}^i$  and  $\hat{\theta}^i$  are the best fit parameter values. The Fisher matrix  $\Gamma_{ij}$  is computed via  $\Gamma_{ij} = (\partial h/\partial\theta^i, \partial h/\partial\theta^j)$  where the brackets in this case indicate the noise weighted inner product. The expected errors in the measurement of the parameter set  $\theta$  is then defined by the square root of the diagonal elements of the inverse Fisher matrix. We follow [20] in our treatment of the parameter estimation analysis for BNS GW signals with the addition of the redshift  $z$  as a parameter. We therefore use  $\theta = (\ln \mathcal{A}, t_c, \phi_c, \ln M_z, \eta, z)$  as our independent parameters where we have absorbed all amplitude information in to a single parameter via  $\tilde{h}(f) = \mathcal{A}f^{-7/6}e^{-i\Psi(f)}$ . The expected SNR of a given BNS signal is dependent upon the nuisance parameters  $\varphi$ . For simplicity we have computed our results assuming an SNR using the ET-B detector design configuration [11] that has been appropriately averaged over

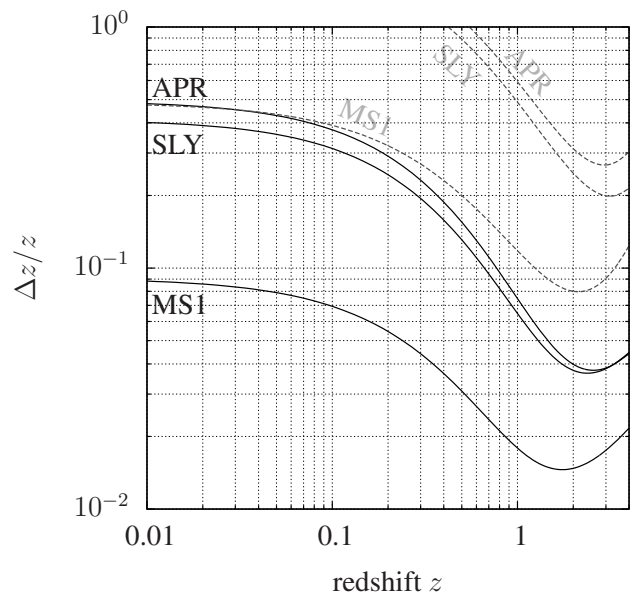


FIG. 1. The fractional uncertainties in the redshift as a function of redshift as obtained from the Fisher matrix analysis for BNS systems using 3 representative EOSs, APR [31], SLY [32] and MS1 [33]. The solid black curves correspond to an analysis that uses the ISCO (as defined in the BNS rest-frame) as the upper cut-off frequency and the dashed grey lines correspond to a fixed rest-frame cut-off frequency of 450 Hz. In all cases the component NSs have rest masses of  $1.4M_{\odot}$  and we have used a cosmological parameter set  $H_0 = 70.5$   $\text{kms}^{-1}\text{Mpc}^{-1}$ ,  $\Omega_m = 0.2736$ ,  $\Omega_k = 0, w_0 = -1$  to compute the luminosity distance for given redshifts. We have assumed detector noise corresponding to the ET-B [34] design (a frequency domain analytic fit to the noise floor can be found in [35]).

each of the 4 constituent angles of  $\varphi$ . The detection range of ET for BNS systems is  $z \approx 1$  for such an angle averaged signal and an SNR threshold of 8. For an optimally oriented system at the same SNR threshold the horizon distance is  $z \approx 4$ .

*Results*—The results of the analysis with respect to the uncertainties in the redshift measurement as a function of redshift are shown in Fig. 1 for a subset of EOSs. We have chosen the following 3 (given in order of increasing  $\lambda$ ) labeled APR [31], SLY [32] and MS1 [33] as realistic representative samples from the set of normal matter (neutron-proton-electron-muon) EOSs. The tidal deformability parameter  $\lambda$  for each EOS has been parameterized as a function of the NS mass as described above and is directly proportional to the level of the tidal phase contribution. We note that Note that for all 3 EOSs, even in our most pessimistic scenario in which the tidal phase cannot be reliably measured beyond 450 Hz (in the BNS rest-frame), the redshift can be measured down to between 10–30% accuracy for sources at  $z \approx 2$ . In the more optimistic case where we are able to model the tidal phase contribution up until ISCO we see uncertainties that span 9–50% for nearby sources ( $z \approx 0.01$ ) which improve to 2–5% at  $z \approx 2$ . The general trend of the results (for all EOSs) is that the fractional redshift uncertainty decreases with

increasing redshift. One would naively assume that lower redshift, stronger signals would allow better determination of parameters, which is the case for the other dimensions of the Fisher analysis ( $\mathcal{M}, \eta, t_c, \phi_c$ ). This effect can be attributed to two factors, the first being that the quantity that is effectively being determined is the ratio between the redshifted and rest mass,  $1+z$ , and hence fractional uncertainties in  $z$  itself will be less discernible at low redshifts. In parallel, as the more distant sources have their waveforms redshifted to lower frequencies, the tidal effects which formally begin at 5PN order and have greatest effect close to the cutoff frequency, are moved towards the most sensitive band of the detector ( $\sim 150$  Hz). From this argument one would conclude that this “sweet spot” would coincide with  $z\sim 10$  and  $z\sim 3$  for ISCO and 450 Hz cut-offs respectively but this effect is diluted at higher redshifts due to a reduction in SNR as the lower frequency part of the signal is lost. We also note the expected trend that the accuracy with which the redshift can be measured improves with increasing  $\lambda$ .

*Discussion*—The analysis presented here is a proof of principle and is based on a number of assumptions and simplifications which we would like to briefly discuss and in some cases reiterate. We feel that our treatment of the current uncertainty in the upper cut-off frequency of the PN waveforms is robust in that although it is unlikely that the approximation is valid up to  $f_{\text{isco}}$ , it is likely that by the 3<sup>rd</sup> generation GW detector era our knowledge of the tidal coupling will have significantly advanced through improved numerical simulations e.g. [36]. The results we present for the 450 Hz rest-frame cut-off frequency should represent a lower limit based on our current level of understanding. We have also neglected the effects of spin in our investigation which we expect to contribute to the PN phase approximation at the level of  $\sim 0.3\%$  [12]. This does not preclude the possibility that the spin parameters may be strongly correlated with the redshift and weaken our ability to determine it. This seems unlikely given the small expected spins in these systems coupled with the relative scalings between the spin terms and the tidal terms,  $x^{-1/2}$  and  $x^{5/2}$  respectively, causing the tidal effects to dominate over spin in the final stage of the inspiral. We also note that the Fisher information estimate of parameter uncertainty is valid in the limit of  $\text{SNR} \gtrsim 10$  [30] and as such, the results at low SNR and hence, those at high  $z$  should be treated as lower limits via the Cramer-Rao bound, on the redshift uncertainty. We also mention here that since the tidal phase corrections are, at leading order, formally of 5<sup>th</sup> PN order we have uncertainty in the effect of the missing PN expansion terms in the BNS waveform between the 3.5PN and 5PN terms. It is comforting to note that as the PN order is increased our results on the redshift uncertainty do converge to the point of  $<1\%$  difference in accuracy between the 3 and 3.5PN terms implying (through extrapolation) that the missing PN terms (as yet not calculated) would not effect our results. Future detailed analysis following this work will complement Fisher based estimates with Monte-Carlo simulations and/or Bayesian posterior based parameter estimation techniques. Similarly, the

signal parameter space should be more extensively explored beyond the canonical  $1.4M_{\odot}$ , equal mass case. In addition, future work will also include BHNS systems which will also contain, encoded within their waveforms, extractable redshift information. Such systems are observable out to potentially higher redshift but tidal effects will become less important as the mass ratio increases [13]. Finally, we briefly mention that GW detector calibration uncertainties in strain amplitude (which for 1<sup>st</sup> generation detectors were typically  $<10\%$ ) will only effect the determination of the luminosity distance. Calibration uncertainties in timing typically amount to phase errors of  $<1^{\circ}$  and would be negligible in the determination of the redshift. Similarly, the effects of weak lensing that would only affect the luminosity distance measurement have been shown to be negligible for ET sources [4].

Current estimates on the formation rate of BNS systems imply that in the 3<sup>rd</sup> generation GW detector era there is the potential for up to  $\sim 10^7$  observed events per year out to redshift  $z \approx 4$  [11]. The results presented here suggest that redshift measurements at the level of  $\sim 10\%$  accuracy can be achieved for *each* BNS event solely from the GW observation. Such systems have long been known as GW standard sirens [1], meaning that the luminosity distance can be extracted from the waveform with accuracy determined by the SNR coupled with the ability with which one is able to infer the geometric orientation of the source. Using a large number of sources all sharing the same redshift, the luminosity distance (free of the orientation parameters) can be determined statistically from the distribution of observed amplitudes. With the ability to extract both the luminosity distance and the redshift out to such cosmological distances and from so many sources the precision with which one could then determine the luminosity distance–redshift relation is significantly enhanced by the sheer number of measurements. Current proposed methods for making cosmological inferences using GW standard sirens [3, 5, 35] rely on coincident EM counterpart signals from their progenitors in order to obtain the redshift. Our method would allow measurements to be made independently of the cosmological distance ladder.

The authors are grateful to J. Veitch, J. Clark, R. Prix, C. Van Den Broeck, B. S. Sathyaprakash, P. Sutton, S. Fairhurst, M. Pitkin, T. Dent, X. Siemens, L. Grishchuk and especially J. Creighton for useful discussions and comments. J. S. Read is supported by NSF grant PHY-0900735.

---

\* chris.messenger@astro.cf.ac.uk

- [1] B. F. Schutz, *Nature (London)*, **323**, 310 (1986).
- [2] D. Eichler, M. Livio, T. Piran, and D. N. Schramm, *Nature (London)*, **340**, 126 (1989).
- [3] S. Nissanke, D. E. Holz, S. A. Hughes, N. Dalal, and J. L. Sievers, *Astrophys. J.*, **725**, 496 (2010), arXiv:0904.1017 [astro-ph.CO].
- [4] B. S. Sathyaprakash, B. F. Schutz, and C. Van Den Broeck, *Classical and Quantum Gravity*, **27**, 215006 (2010),

- arXiv:0906.4151 [astro-ph.CO].
- [5] W. Zhao, C. Van Den Broeck, D. Baskaran, and T. G. F. Li, *Phys. Rev. D*, **83**, 023005 (2011), arXiv:1009.0206 [astro-ph.CO].
- [6] J. Abadie *et al.*, *Nuclear Instruments and Methods in Physics Research A*, **624**, 223 (2010), arXiv:1007.3973 [gr-qc].
- [7] H. Grote and the LIGO Scientific Collaboration, *Classical and Quantum Gravity*, **25**, 114043 (2008).
- [8] F. Acernese *et al.*, *Classical and Quantum Gravity*, **25**, 184001 (2008).
- [9] G. M. Harry and the LIGO Scientific Collaboration, *Classical and Quantum Gravity*, **27**, 084006 (2010).
- [10] J. Abadie *et al.*, *Classical and Quantum Gravity*, **27**, 173001 (2010), arXiv:1003.2480 [astro-ph.HE].
- [11] M. Abernathy *et al.*, “Einstein gravitational wave telescope conceptual design study,” (2011).
- [12] T. Hinderer, B. D. Lackey, R. N. Lang, and J. S. Read, *Phys. Rev. D*, **81**, 123016 (2010), arXiv:0911.3535 [astro-ph.HE].
- [13] F. Pannarale, L. Rezzolla, F. Ohme, and J. S. Read, *ArXiv e-prints* (2011), arXiv:1103.3526 [astro-ph.HE].
- [14] E. E. Flanagan and T. Hinderer, *Phys. Rev. D*, **77**, 021502 (2008).
- [15] J. S. Read, C. Markakis, M. Shibata, K. Uryū, J. D. E. Creighton, and J. L. Friedman, *Phys. Rev. D*, **79**, 124033 (2009), arXiv:0901.3258 [gr-qc].
- [16] J. S. Bloom, S. R. Kulkarni, and S. G. Djorgovski, *Astron. J.*, **123**, 1111 (2002), arXiv:astro-ph/0010176.
- [17] E. Nakar, *Physics Reports*, **442**, 166 (2007), arXiv:astro-ph/0701748.
- [18] L. Rezzolla, B. Giacomazzo, L. Baiotti, J. Granot, C. Kouveliotou, and M. A. Aloy, *Astrophys. J. Lett.*, **732**, L6+ (2011), arXiv:1101.4298 [astro-ph.HE].
- [19] C. Cutler and É. E. Flanagan, *Phys. Rev. D*, **49**, 2658 (1994), arXiv:gr-qc/9402014.
- [20] K. G. Arun, B. R. Iyer, B. S. Sathyaprakash, and P. A. Sundararajan, *Phys. Rev. D*, **71**, 084008 (2005), arXiv:gr-qc/0411146.
- [21] S. V. Dhurandhar and B. S. Sathyaprakash, *Phys. Rev. D*, **49**, 1707 (1994).
- [22] K. G. Arun, B. R. Iyer, B. S. Sathyaprakash, and P. A. Sundararajan, *Phys. Rev. D*, **72**, 069903 (2005).
- [23] J. Vines, E. E. Flanagan, and T. Hinderer, *Phys. Rev. D*, **83**, 084051 (2011).
- [24] T. Hinderer, *Astrophys. J.*, **677**, 1216 (2008), arXiv:0711.2420.
- [25] A. W. Steiner, J. M. Lattimer, and E. F. Brown, *Astrophys. J.*, **722**, 33 (2010), arXiv:1005.0811 [astro-ph.HE].
- [26] F. Özel, G. Baym, and T. Güver, *Phys. Rev. D*, **82**, 101301 (2010), arXiv:1002.3153 [astro-ph.HE].
- [27] T. Damour and A. Nagar, *Phys. Rev. D*, **80**, 084035 (2009), arXiv:0906.0096 [gr-qc].
- [28] K. D. Kokkotas and G. Schafer, *Mon. Not. R. Astron. Soc.*, **275**, 301 (1995), arXiv:gr-qc/9502034.
- [29] R. A. Fisher, **123**, 866 (1925).
- [30] M. Vallisneri, *Phys. Rev. D*, **77**, 042001 (2008), arXiv:gr-qc/0703086.
- [31] A. Akmal, V. R. Pandharipande, and D. G. Ravenhall, *Phys. Rev. C*, **58**, 1804 (1998), arXiv:hep-ph/9804388.
- [32] F. Douchin and P. Haensel, *Astronomy & Astrophysics*, **380**, 151 (2001), arXiv:astro-ph/0111092.
- [33] H. Müller and B. D. Serot, *Nuclear Physics A*, **606**, 508 (1996), arXiv:nucl-th/9603037.
- [34] S. Hild, S. Chelkowski, and A. Freise, *ArXiv e-prints* (2008), arXiv:0810.0604 [gr-qc].
- [35] C. K. Mishra, K. G. Arun, B. R. Iyer, and B. S. Sathyaprakash, *Phys. Rev. D*, **82**, 064010 (2010), arXiv:1005.0304 [gr-qc].
- [36] K. Hotokezaka, K. Kyutoku, H. Okawa, M. Shibata, and K. Kiuchi, *Phys. Rev. D*, **83**, 124008 (2011), arXiv:1105.4370 [astro-ph.HE].